

LWT

Volume 113, October 2019, 108332

**STRUCTURAL CHANGES ASSOCIATED WITH THE INACTIVATION OF
LIPOXYGENASE BY PULSED LIGHT**

José Antonio Pellicer^a, Patricia Navarro^a, Pilar Hernández Sánchez^a and Vicente M. Gómez-López^b

^aDepartamento de Ciencia y Tecnología de Alimentos, Universidad Católica de Murcia (UCAM), Campus de los Jerónimos 135, Guadalupe 30107, Murcia, Spain.

^bCátedra Alimentos para la Salud, Universidad Católica de Murcia (UCAM), Campus de los Jerónimos 135, Guadalupe 30107, Murcia, Spain.

<https://doi.org/10.1016/j.lwt.2019.108332>

© <2019>. This manuscript version is made available under the CC-BY-NC-ND 4.0 license <http://creativecommons.org/licenses/by-nc-nd/4.0/>

**STRUCTURAL CHANGES ASSOCIATED WITH THE INACTIVATION OF
LIPOXYGENASE BY PULSED LIGHT**

José Antonio Pellicer^a, Patricia Navarro^a, Pilar Hernández Sánchez^a and Vicente M. Gómez-López^b

^aDepartamento de Ciencia y Tecnología de Alimentos, Universidad Católica de Murcia (UCAM), Campus de los Jerónimos 135, Guadalupe 30107, Murcia, Spain.

^bCátedra Alimentos para la Salud, Universidad Católica de Murcia (UCAM), Campus de los Jerónimos 135, Guadalupe 30107, Murcia, Spain.

Corresponding author:

Vicente M. Gómez-López, phone: + 34 968 278 638, vmgomez@ucam.edu

ABSTRACT

Pulsed light (PL) is a non-thermal technology able to inactivate enzymes. Lipoxygenase (LOX) causes enzymatic rancidity in some foods. This study aimed to determine the structural changes associated with the PL inactivation of LOX and used measurements of residual activity, temperature, spectropolarimetry, fluorescence, spectrophotometry, free sulfhydryl and carbonyl contents and electrophoresis. LOX inactivation was non-log-linear, with a slight temperature rise. PL significantly increased the concentration of carbonyls and free-sulfhydryls of LOX and caused loss of ellipticity and intrinsic fluorescence, a red shift in the intrinsic fluorescence peak and an increase in **1-anilino-8-naphthalenesulfonate** fluorescence. The turbidity of LOX sample increased during inactivation and electrophoretic bands faded. Phase diagram analysis showed no evidence of formation of intermediates. In summary, the inactivation of LOX by PL followed a Weibull kinetics, is exclusively photochemical and is an all-or-none process where the protein gets oxidized, decreases its α -helix content, unfolds and aggregates.

Keywords: pulsed light; **lipoxygenase inactivation**; **enzyme** structure, soybean.

1. Introduction

Pulsed light (PL) is a non-thermal technology based in the application of short pulses of high-energy polychromatic light spanning from infrared to UV light, in which the UV-C part of the spectrum accounts for many of its effects (Gómez-López, Ragaert, Debevere, & Devlieghere, 2007). Initially adopted by food technologists for microbial inactivation, its application to protein treatment has been explored in recent years. This includes goals such as allergenicity abatement (Shriver & Yang, 2011), modification of functional properties (Fernández, Artiguez, Martínez de Marañón, Villate, Blanco, & Arboleya, 2012) and enzyme inactivation (Manzocco, Panozzo, & Nicoli, 2013a). The inactivation of enzymes by PL was initially described in the pioneering patent by Dunn et al. (1989). In the peer-reviewed literature, Manzocco et al. (2013a) first reported the inactivation of a food enzyme by PL, namely polyphenol oxidase (PPO). Later on, the inactivation of other enzymes such as alkaline phosphatase (Innocente et al., 2014), lipoxygenase (Janve, Yang, Marshall, Reyes-De-Corcuera, & Rababah et al., 2014), peroxidase (POD) (Wang, Zhang, Venkitasamy, Wu, Pan, & Ma, 2017; Pellicer & Gómez-López, 2017), a commercial protease (Arroyo, Kennedy, Lyng, & O'Sullivan, 2017) and polygalacturonase (Pellicer, Navarro, & Gómez-López, 2019) have been studied. The structural changes caused by PL on enzymes that help to understand how they are inactivated have been studied with different level of detail, from the simple report of inactivation curves (no structural studies) to deeper studies reporting changes in different structural levels (Pellicer & Gómez-López, 2017). As any other photochemical process, pulsed light effects are governed by the laws of photochemistry and photophysics. The unit used to characterize a photochemical process is fluence (J/m^2) as defined by IUPAC nomenclature (Braslavsky, 2007) and there is no special reason to consider PL as a special case within photochemical sciences in which fluence should not be used. Factors such as

distance from light source to target, treatment time, number of pulses and discharge voltage are just variables influencing fluence, which is the only unit that allows interlaboratory comparisons and scaling-up (Gómez-López, & Bolton, 2016). Fluence is widely used for characterization of processes driven by continuous wave UV light, which is an industrially consolidated technology, but it is still less used to characterize PL processes. Perhaps, the lack of a standardized procedure for fluence dosimetry in PL tests and its required equipment accounts for the lack of wide acceptance. A protocol to cope with this issue has been recently proposed (Gómez-López, & Bolton, 2016). The protocol goes a step beyond, proposing photon irradiance (Einstein/m² s) instead of fluence as unit for PL process characterization. This method is largely based in the protocol recently proposed (Bolton, Linden, & Mayor-Smith, 2015) for CW UV light technology, and while the use of photon irradiance is pending for acceptance, the use of fluence is accepted and can be still used.

Lipoxygenase (LOX; EC 1.13.11.12) is a non-heme iron containing enzyme that catalyzes the deoxygenation of fatty acids containing one or more (1Z, 4Z)-pentadiene systems (Minor et al., 1996). Plant LOXs are classified as LOX-1, LOX-2 and LOX-3 (Youn, Sellhorn, Mirchel, Gaffney, Grimes, & Kang, 2006). LOX-1 extracted from soybean seed is the most studied isoenzyme. LOX-1 structure consists of a single polypeptide chain of 839 aminoacid residues and can be separated in two domains. The smaller N-terminal β -barrel domain comprises the NH₂-terminal residues 1-146. The large principally helical C-domain comprises residues 147-839 and includes the catalytic Fe-binding site (Minor et al., 1996).

LOX is ubiquitous in plants and its activity affects the stability of some foods. The inactivation of LOX in foods is very important because it catalyzes the oxidation of unsaturated fatty acids, causing undesirable flavors. The deleterious effects of LOX on

foods have been summarized by Chedea & Jisaka (2011), and include undesirable flavours in protein products derived from legume seeds, stale flavor in beers and co-oxidation of carotenoids, which discolors foods and reduce their nutritional quality. The beany flavor is the principal defect of many soybean products and is caused by some ketones and aldehydes produced through LOX-catalyzed oxidation of soybean oil (Berk, 2019). LOX inactivation is traditionally achieved by heating, but thermal processing causes deleterious effects in vegetable quality. Therefore, effective non-thermal methods are desired and PL could be one of them.

The capability of PL to inactivate LOX was first demonstrated by Janve et al. (2014) and some factors influencing its inactivation have also been studied (Alhendi, Yang, & Sarnoski, 2018). The main findings reported in this work are that LOX inactivation by PL follows a first-order kinetic and is consequence of protein fragmentation, ruling out the possibility of aggregation. Once this interesting application of PL has been developed, we believe that a deeper study of the structural changes associated to LOX inactivation by PL is deserved. Therefore, the aim of this work was to study the structural changes associated to LOX inactivation by PL, including inactivation kinetics and also potential aggregation measured by spectrophotometry, and features of the inactivation process that have not been reported before, namely: changes in secondary and tertiary structure, protein oxidation and free sulfhydryl concentration, as well phase diagram analysis.

2. Materials and methods

2.1. Reagents

Type I lipoxygenase from soybean (L7395, Sigma-Aldrich), linoleic acid, 1-anilino-8-naphthalenesulfonate (ANS), Tween 20, dithiobisnitrobenzoic acid (DTNB, Ellman's reagent), tris(hydroxymethyl)aminomethane (TRIS), phosphate buffers and guanidine

HCl were purchased from Sigma-Aldrich (St. Louis, MO, USA). 2,4-dinitrophenylhydrazine (DNPH), HCl, methanol and acetic acid were purchased from Scharlau (Barcelona, Spain). Products used in electrophoresis were acquired from Biorad (California, USA), they were: 30 % acrylamide/bis-acrylamide (29:1) solution, ammonium persulfate, tetramethylethylenediamine (TEMED), native sample buffer, electrophoresis cuvette and Coomassie Blue. Boric acid was from Guinama (Valencia, Spain) and trichloroacetic acid (TCA) from Panreac (Barcelona, Spain).

A 0.4 mg/mL (4.23 μ M) LOX solution in 0.01 M Tris-HCl buffer, pH 9, was prepared. LOX source, concentration, buffer and pH were selected to have similar conditions than those used by Janve et al. (2014). However, the treatment conditions were not exactly the same due to the differences in PL systems and because those authors did not report the fluence applied in their experiments, which is required for result comparisons. LOX concentration was the same in all experiments and analytical determinations. In this way, enzyme concentration effects were ruled out and the results of the different structural determinations can be correlated with the inactivation curve. It has been demonstrated that the inactivation curves of enzymes by PL treatments are influenced by enzyme concentration (Manzocco et al., 2013a); this effect has also been detected specifically for LOX (Alhendi et al., 2018).

2.2. Pulsed light treatment and temperature measurement

Pulsed light treatment and temperature measurement were carried out as described previously (Pellicer & Gómez-López, 2017). Twenty ml of enzyme preparation placed in a Petri dish without cover was treated with PL in a XeMaticA-Basic-1L unit (Steribeam, Kehl, Germany) operated at 2.5 kV, which generates a light pulse of 200 μ s with an energy of 500 J/pulse, which contains 21 % of UV component and a characteristic emission spectrum similar to one previously reported (Cudemos, Izquier, Medina-

Martinez, & Gómez-López, 2013). The distance lamp-liquid surface was 6.7 cm and the dish was centred exactly below the middle of the lamp length. The enzyme preparation was homogenised between pulses by a stirrer (Topolino, IKA, Staufen, Germany) that supported the Petri dish, which was placed inside the treatment chamber of the PL system. Samples were withdrawn at different time intervals for analytical determinations.

Fluence dosimetry was carried out by an oscilloscope (PC-Lab 2000 LT PC, Velleman, Belgium). The light fluence per pulse ($F_{o,\pi}$) at sample surface was 2.14 J/cm². Higher fluences were achieved by applying multiple pulses until a maximum of 45 pulses, according to the equation:

$$F_o = F_{o,\pi} n$$

where F_o is the fluence (J/cm²) delivered to sample surface and n the number of pulses.

Sample temperature was measured by using an infrared thermometer (ScanTemp 410, TFA, Germany) according to Pellicer and Gómez-López (2017).

2.3. Enzymatic activity

The substrate was freshly prepared according to a modified method of Axelrod, Cheesbrough and Laakso (1981). Tween 20 (50 µL) and an equal part of linoleic acid were homogenized with 0.2 M borate buffer (500 µL), pH 9.0 and 0.5 N NaOH to yield a clear solution. LOX activity was measured during 20 seconds from the slope of the absorbance at 234 nm vs time plot by means of an UV-Vis spectrophotometer (UV-1700, Shimadzu, Japan) at 25 °C; the lag phase was excluded when present. The reaction mixture was composed by 0.933 mL borate buffer (0.2 M, pH 9), 0.05 mL substrate solution and 0.017 mL LOX, for a final volume of 1 mL. For low residual LOX activity, the sample volume was increased to a maximum of 0.17 mL by reducing buffer volume.

The blank for spectrophotometric measurements was prepared in the same way as the

reaction mixture but replacing the enzyme by the buffer. Results were expressed in terms of relative activity (RA), which was defined as:

$$RA = A/A_0$$

where A is the residual activity and A_0 the enzymatic activity before treatment.

Results were fitted to a first-order inactivation kinetics as well as the Weibull model.

The first-order inactivation kinetics is described by the following equation:

$$\ln RA = -k F$$

where k is the first-order inactivation rate and F the fluence (J/cm^2).

The Weibull model reads as:

$$\log RA = - \left(\frac{F}{\alpha} \right)^\beta$$

where α (J/cm^2) is a scale parameter and β a shape parameter.

2.4. Far-UV circular dichroism

Far-UV circular dichroism (CD) spectra were recorded by a PiStar-180 Spectrometer (Applied Photophysics, Leatherhead, United Kingdom) using a 1 mm path-length rectangular quartz cuvette at 20 °C. The number of samples per wavelength was automatically set by the equipment by adaptive sampling using a signal-to-noise ratio of 0.01. The molecular mass of the enzyme and its number of aminoacids, which are required to transform ellipticity values from millidegrees to mean residual molar ellipticity were taken from protein data bank for the LOX coded 1YGE (PDB, 2019), which is based on data deposited by Minor et al. (1996). Data deconvolution was carried out BestSel software with a scale factor of 3.8 (Micsonai et al., 2015).

2.5. Steady-state intrinsic fluorescence

Intrinsic tryptophan fluorescence was measured as described before, as well as calculations of parameter A and the phase diagram (Pellicer & Gómez-López, 2017) but measuring every five pulses up to 45 pulses. In brief, intrinsic tryptophan fluorescence was measured at an excitation wavelength (λ_{ex}) of 293 nm and an emission wavelength (λ_{em}) range of 300-450 nm, in a spectrofluorimeter (RF-Shimadzu, Japan) with a quartz cuvette of 1 cm optical path at 25 °C.

The fluorescence spectra were also analyzed using spectral center of mass according to the following equation:

$$\lambda_{av} = \sum \lambda F(\lambda) / \sum F(\lambda)$$

where λ_{av} is the center of mass (nm) and $F(\lambda)$ is the fluorescence at wavelength λ .

2.6. ANS fluorescence

In order to study the binding of hydrophobic dye ANS, protein samples were incubated for 30 min at 25 °C in the dark with appropriate amount of ANS, in 0.1M phosphate buffer (pH 6.5), to give a 50-fold molar excess. The fluorescence of ANS was excited at 385 nm and emission was collected between 400 and 660 nm, at 25 °C. Measurements in the absence of the protein were also carried out in order to visualize fluorescence intensities from unbound ANS.

2.7. UV-vis spectrometry

UV-vis spectra were recorded in the UV-1700 spectrophotometer using a quartz cuvette with a 1 cm path length at 25 °C. Data for determining turbidity and aggregation index were extracted from these spectra. Turbidity was measured as absorbance at 420 nm (Ju & Kilara, 1998). The aggregation index (AI) was calculated from the following equation (Katayama et al., 2005):

$$AI = 100 \cdot A_{340} / (A_{280} - A_{340})$$

where A_{340} and A_{280} are the absorbance's at 340 and 280 nm respectively.

2.8. Free-sulphydryl content

Free sulphydryl content was determined by the method of Ellman (Ellman, 1959) as modified by Siddique, Maresca, Pataro, and Ferrari (2017), but using an enzyme concentration of 0.4 mg/mL. In brief, 2.75 mL of enzyme solution was mixed with 0.25 mL of a 1 g/L of Ellman's reagent in 50 mM Tris-HCl buffer. The solution was incubated for 30 min at room temperature in darkness. Then, the absorbance of the solution was measured at 412 nm. Samples were measured every 15 pulses.

The concentration of free sulphydryl's was calculated according to (Beveridge, Toma, & Takai, 1974):

$$\frac{\mu M SH}{g} = \frac{73.53 A_{412} D}{C} \quad (2)$$

where A_{412} is the absorbance at 412 nm, D stands for the dilution factor, C is the sample concentration (mg enzyme/mL) and 73.53 is derived from $10^6 / (1.36 \times 10^4)$. 10^6 is a conversion factor and $1.36 \times 10^4 / M \text{ cm}$ is the molar absorptivity.

2.9. Carbonyl groups

Protein carbonyl groups were determined based on the method by Oliver, Ahn, Moerman, Goldstein, and Stadtman (1987) modified by Fernández, Ganan, Guerra and Hierro (2014) with some adaptations. Enzyme samples (4 mL) were divided in equal aliquots and precipitated with 10 % TCA final concentration. One aliquot was mixed with an equal volume of 2 N HCl and the other mixed with an equal volume of 0.2 % DNPH in 2 N HCl. Both samples were incubated at 30 °C for 60 min with vortexing every 10 min. The samples were precipitated once more with TCA and centrifuged at 2000 g for 10 min and

then, extracted twice with ethanol:ethyl acetate (1:1, v/v) and precipitated again with TCA. The supernatants were removed and the pellets were dissolved in 6 M guanidine-HCl with 20 mM sodium phosphate buffer, pH 6.5 with 10 min vortexing. Carbonyl contents were determined from the absorbance at 370 nm using an extinction coefficient of 21,000/M cm.

2.10. Electrophoresis

For electrophoresis, the separating gel (8 %) was prepared by mixing acrylamide, ammonium persulfate and TEMED. The mixture was put inside the gap between the glass plates. After complete polymerization, the stacking gel (4%) was prepared using ammonium persulfate and TEMED. The protein samples (0, 15, 30 and 45 light pulses) were mixed with native sample buffer and loaded into the wells, using an appropriate voltage (120 V for 50 min) to run the electrophoresis. **Standards were run together with the samples, they were: horse ferritin (450 kDa), bovine catalase (240 kDa), rabbit aldolase (160 kDa), bovine serum albumin (67 kDa) and egg albumin (45 kDa), all from SERVA electrophoresis GmbH (Heidelberg, Germany).** Spots were revealed by Coomassie Blue R-250 dissolved in 45% methanol, 10% acetic acid and 45% water, and slowly shake it on horizontal rotator for 60 minutes. Then, the gel was placed in the destaining solution (20% methanol, 10% acetic acid and 70% water) under shaking for 60 minutes, replacing the destaining solution until clear bands were observed.

2.11. Statistical analysis

Results were analyzed for statistical differences by one-way ANOVA and Tukey's test, with $p < 0.05$, by using SPSS Statistics 24 (IBM, USA).

3. Results and discussion

3.1. Inactivation kinetics

Initial LOX activity was $136 \pm 10 \mu\text{M}$ of conjugated diene/minute and decreased during PL treatment until negligible levels ($< 1\%$ RA) with the application of 96 J/cm^2 (fig. 1). Since photochemical enzyme inactivation is considered to follow a first-order kinetics, a first attempt to fit data to that kinetics was assayed. However, the plot of $\ln \text{RA}$ vs fluence clearly departed from a straight line, which R^2 was only 0.9255. The Weibull model fits data better than the first-order kinetics, with a $R^2 = 0.9865$ and a root mean sum of squared error of 0.2240. Weibull parameters were: $\alpha = 42.73 \text{ J/cm}^2$ and $\beta = 1.90$, with a predicted $\log \text{RA}_0 = -0.13$. These results are limited to our experimental conditions, for example, a thicker layer of enzyme solution should yield a slower inactivation due to light attenuation through the liquid column. The Weibull model has also found to be the best to fit the inactivation of polyphenol oxidase by PL (Pellicer, Navarro, & Gómez-López, 2018). The deviation of the first-order kinetics might be due to the co-existence of isoenzymes with different susceptibility to PL treatment. A supposedly pure isoenzyme was used in the current work, which was the same used by Janve et al. (2014). However, it is possible that the enzyme source used in this work contains several isoenzymes since the supplier (Sigma-Aldrich, 2019) declares that six bands have been identified by isoelectric focusing in its LOX powder but it has not been determined if they represent isoenzymes. Electrophoresis results reported hereby (fig. 2) and by Janve et al. (2014) do not reveal the presence of isoenzymes; the differences in both separation methods can account for this discrepancy.

The electrophoresis of the protein solution shows one band between the molecular weight markers of 67 and 160 kDa for the untreated solution (Fig. 2), which corresponds to native LOX-1. PL treatment made this band fade and no other bands appeared in the gel for

native and treated enzyme, which is consistent with the loss of activity observed in fig. 1 and it was also noticed by Janve et al. (2014).

Sample temperature (Table 1) was 24.5 ± 1.1 °C at the beginning of the experiments and rose to 30.0 ± 1.3 °C after applying 45 pulses. This implies a temperature increase of less than 6 °C, which allows to rule out any heat contribution to the observed inactivation, leading to consider LOX inactivation by PL purely a photochemical phenomenon.

3.2. Far-UV circular dichroism

Circular dichroism is an analytical tool that allows studying the secondary structure of proteins. The far-UV circular dichroism spectrum of the native LOX has the typical features of a protein with substantial proportion of α -helical structure (fig. 3a); those are, a negative peak at 208 nm and a shoulder at 222 nm. According to protein data bank (PDB, 2019) with data supplied by (Minor et al., 1996), LOX-1 contains 41 % of α -helix and 14 % β -sheet. Spectra of the PL treated LOX shows a gradual decrease of the shoulder at 222 nm characteristic of a progressive loss of α -helical structure. Deconvoluted analysis shows (fig. 3b) a progressive decrease of α -helix during the course of the PL treatment, and an increase of β -sheet, β -turn and disordered regions. Similar changes have been reported for PL treated POD (Pellicer & Gómez-López, 2017).

3.3. Free SH groups content

The determination of free SH groups content by means of the Ellman's reagent requires contact between these groups and the reagent. SH groups can be hidden from contact with the Ellman's reagent by either being part of disulfide bridges or by being buried in the inner core of the protein. Therefore, an increase in the detection of free SH groups is related to cleavage of disulfide bridges and/or protein unfolding. The first reasoning has been used to explain the increase of SH groups observed by treating egg white by PL

(Manzocco, Panozzo, & Nicoli, 2013b), while the second one has been used to explain results observed after treating whey protein isolate by PL (Siddique et al., 2017). A progressive and statistically significant ($p < 0.05$) increase of free sulfhydryl group content of LOX has been observed during the course of PL treatment (Table 2). LOX-1 contains four Cys residues (PDB, 2019). However, it is admitted that has no disulfide bridges and its cysteine residues are rather inaccessible to compounds such as the Ellman's reagent (Sudharshan & Rao, 1999). Therefore, in the current case, the increased in free sulfhydryl groups are a consequence of enzyme unfolding, leading to a higher exposure of free sulfhydryls to the environment, which become accessible to the Ellman's reagent. This change has also been observed when LOX-1 has been denatured by urea (Sudharshan & Rao, 1999). Besides indicating LOX-1 unfolding, higher free SH content increase the possibility of protein aggregation. Exposed free sulfhydryl groups are very reactive and can react with other free sulfhydryl groups of the same molecule or other molecules, the latter possibility lead to formation of aggregates, as observed by Elmnasser et al. (2008) for PL treated β -lactoglobulin.

3.4. Intrinsic fluorescence and spectral center of mass

The fluorescence of tryptophan is the most common fluorescence internal probe used to determine changes in tertiary structure. LOX-1 has 13 Trp residues (PDB, 2019), most of them located in hydrophobic regions (Malvezzi-Campeggi, Rosato, Finazzi-Agrò and Maccarrone, 2001). Fig. 4a shows the change in tryptophan fluorescence with the course of PL treatment. PL causes a decrease in fluorescence signal as consequence of the exposure of tryptophan residues, initially buried in the hydrophobic core of the molecule, to the external hydrophilic ambient as consequence of its unfolding. The quantum yield of tryptophan is lower when exposed to a hydrophilic ambient in comparison with it is in a hydrophobic ambient, therefore, the fluorescence decreases when protein unfolds

(Ionitã, Stãnciuc, Aprodu, Rãpeanu, & Bahrim, 2014). This result is in harmony with previous reports on enzyme inactivation by PL (Pellicer et al., 2018, 2019). Complementarily, the spectral center of mass (fig. 4b) allows a better distinction of wavelength shifts at the peak fluorescence. PL treatment caused an 8-nm red shift in the tryptophan fluorescence of LOX at the end of the treatment. Both, the change in fluorescence intensity and the red shift are characteristics of protein unfolding (Ionitã et al., 2014).

3.5. Parameter A and phase diagram

Enzyme inactivation can be an all-or-none process consisting in a native enzyme that undergoes inactivation, giving place to a protein with no catalytic activity **in a single step**, or can be a multistep process where the formation of a non-catalytic protein is preceded by one or more intermediates. Parameter A and phase diagram allow revealing the existence of intermediates. Parameter A reflects the shape and position of a fluorescence spectrum and allows monitoring the unfolding pathways of proteins (Jiang, Su, Zhang, Wei, Yan, & Zhou, 2008). In the phase diagram, a straight line reflects an all-or-none process while several straight lines indicate a multistep process (Kuznetsova, Turoverov, & Uversky, 2004).

Parameter A (Fig. 4c) as well as phase diagram (Fig. 4d) show linear changes in the course of the inactivation, without any indication of the formation of intermediates. Therefore, it can be concluded that the inactivation of LOX-1 by PL is an all-or-none process.

3.6. ANS fluorescence

ANS is a common fluorescence external probe used to monitor protein unfolding. Its fluorescence emission is increased upon binding to solvent exposed hydrophobic clusters (Stãnciuc, Aprodu, Rãpeanu, & Bahrim, 2012). Our results (fig. 5) show that the

fluorescence of ANS progressively increases during the course of LOX-1 inactivation by PL. The fluorescence emission spectrum shows a significant 37 nm blue-shift between the peaks of free and bound ANS indicating a major exposure of the internal non-polar groups to water (Dumitraşcu, Stănciuc, Bahrim, Ciurac, & Aprodu, 2016). The blue shift is consequence of induced intramolecular charge transfer of ANS when it binds to protein (Gasymov & Glasgow, 2007). This kind of result is a clear indicator of protein unfolding and it is in line with the results reported hereby for intrinsic fluorescence changes.

3.7. Enzyme aggregation

Proteins undergoing an inactivation process may aggregate, which causes changes in their UV-vis spectrum useful to identify this phenomenon. Aggregation can occur *via* formation of disulfide bridges between free sulfhydryl's, as reported by Elmnasser et al. (2018) for PL treated β -lactoglobulin; or hydrophobic interactions between hydrophobic parts of the molecules that are in the inner part of the protein before inactivation. Both, the aggregation index and the turbidity (Table 1) linearly increase during PL treatment with statistically significant differences ($p < 0.05$), indicating the formation of aggregates. The aggregates should occur *via* hydrophobic interactions because there is no indication of possible formation of intra-molecular disulfide bridges. The increase of free sulfhydryl groups followed by a decrease is taken as an indicator of generation of disulfide bridges, where a higher exposure of sulfhydryl groups after cysteine cleavage or protein unfolding during early stages of the treatment is followed by formation of inter- or intramolecular disulfide bridges. For example, in egg white proteins, free sulfhydryl groups increased up to nine light pulses, then decreased sharply after 12 pulses, which has been correlated with the formation of protein aggregates (Manzocco et al., 2013b). In the current case, no decrease of free sulfhydryl's was observed (Table 2) after its early increase, which leaves hydrophobic interactions as the only possibility to explain the observed aggregation.

Aggregation of proteins require that they collide among them and the probability of collision increases with concentration, therefore, the values for turbidity and aggregation index reported in this work are only valid for the enzyme concentration that was used.

3.8. Carbonyl groups

Protein-bound carbonyl content is the most frequently used marker of protein oxidation. Increasing carbonyl groups are an important indicator of enzyme destabilization since they indicate a change in primary structure. Protein-bound carbonyl content has previously been used to determine the oxidation of bovine serum albumin (Fernández et al., 2014) and whey protein isolate (Siddique et al., 2016) treated by PL. LOX-1 is oxidized by PL (Table 2), with a statistically significant ($p < 0.05$) increase in carbonyl content during the course of the treatment.

4. Conclusion

The structural changes associated with LOX inactivation by PL were determined. Under our working conditions, the inactivation of LOX by PL follows a Weibull kinetics, is exclusively a photochemical effect and an all-or-none process. PL causes the oxidation of aminoacids and decreases the α -helix content of LOX. LOX unfolds during PL treatment as deducted from observed changes in intrinsic and extrinsic fluorescence and free-sulfhydryl content. The protein aggregates during treatment, likely due to hydrophobic interactions. Information from this research should help to a better understanding of the enzyme inactivation process by PL and would provide a stronger background for the practical implementation of this technology.

Conflict of interest

The authors have declared no conflict of interest.

Acknowledgments

Dr. César Flores (ACTI, Universidad de Murcia) for his assistance in circular dichroism determinations.

This work was supported by Universidad Católica de Murcia, grant PMAFI/29/14.

References

Alhendi, A., Yang, W., Sarnoski, P. J. (2018). The effect of solution properties on the photochemical ability of pulsed light to inactivate soybean lipoxygenase. *Int. J. Food Eng.* 20180086. <http://dx.doi.org/10.1515/ijfe-2018-0086>.

Arroyo, C., Kennedy, T. m., Lyng, J. G., & O'Sullivan, M. (2017). Comparison of conventional heat treatment with selected non-thermal technologies for the inactivation of the commercial protease Protamex™. *Food and Bioproducts Processing*, 105, 95-103. <http://dx.doi.org/10.1016/j.fbp.2017.06.004>.

Axelrod, B., Cheesbrough, T. M., & Laakso, S. (1981). Lipoxygenase from soybeans: EC 1.13. 11.12 Linoleate: oxygen oxidoreductase. In *Methods in enzymology* (Vol. 71, pp. 441-451). Academic Press.

Berk, Z. 2019. <http://www.fao.org/docrep/t0532e/t0532e01.htm>. Accessed 11 April 2019.

Beveridge, T., Toma, S. J., & Nakai, S. (1974). Determination of SH- and SS-groups in some food proteins using Ellman's reagent. *Journal of Food Science*, 39, 49-51. <https://doi.org/10.1111/j.1365-2621.1974.tb00984.x>

Bolton, J. R., Linden, K. G., & Mayor-Smith, I. (2015). Rethinking the concepts of fluence (UV dose) and fluence rate: the importance of photon-based units—a systemic review. *Photochemistry and Photobiology*, *91*, 1252–1262. <http://doi:10.1111/php.12512>.

Braslavsky, S. E. (2007). Glossary of terms used in photochemistry. *Pure & Applied Chemistry*, *79*, 293–465. <http://doi:10.1351/pac200779030293>.

Chedea, V. S., & Jisaka, M. (2011). Inhibition of soybean lipoxygenases—Structural and activity models for the lipoxygenase isoenzymes family. In *Recent Trends for Enhancing the Diversity and Quality of Soybean Products*, Dora Krezhova (Ed.), ISBN: 978-953-307-533-4, InTech.

Cudemos, E., Izquier, A., Medina-Martinez, M. S., & Gómez-López, V. M. (2013). Effects of shading and growth phase on the microbial inactivation by pulsed light. *Czech Journal of Food Science*, *31*(2), 189-193. <https://doi.org/10.17221/145/2012-CJFS>

Dumitraşcu, L., Stănciuc, N., Bahrim, G. E., Ciumac, A., & Aprodu, I. (2016). pH and heat-dependent behaviour of glucose oxidase down to single molecule level by combined fluorescence spectroscopy and molecular modelling. *Journal of the Science of Food and Agriculture*, *96*, 1906-1914. <https://doi.org/10.1002/jsfa.7296>

Dunn, J. E., Clark, R. W., Asmus, J. F., Pearlman, J. S., Boyer, K., Painchaud, F., & Hofmann, G. A. (1989). U.S. Patent No. 4,871,559. Washington, DC: U.S. Patent and Trademark Office.

Ellman, G. L. (1959). Tissue sulfhydryl groups. *Archives of Biochemistry and Biophysics*, *82*, 70-77. [https://doi.org/10.1016/0003-9861\(59\)90090-6](https://doi.org/10.1016/0003-9861(59)90090-6)

Elmnasser, N., Dalgalarrrondo, M., Orange, N., Bakhrouf, A., Haertlé, T., Federighi, M., & Chobert, J. M. (2008). Effect of pulsed-light treatment on milk proteins and lipids.

Journal of Agricultural and Food Chemistry, 56, 1984-1991. <http://doi.org/10.1021/jf0729964>.

Fernández, E., Artiguez, M. L., de Marañón, I. M., Villate, M., Blanco, F. J., & Arboleya, J. C. (2012). Effect of pulsed-light processing on the surface and foaming properties of β -lactoglobulin. *Food Hydrocolloids*, 27, 154-160. <https://doi.org/10.1016/j.foodhyd.2011.08.001>

Fernández, M., Ganan, M., Guerra, C., & Hierro, E. (2014). Protein oxidation in processed cheese slices treated with pulsed light technology. *Food Chemistry*, 159, 388-390. <https://doi.org/10.1016/j.foodchem.2014.02.165>

Gasymov, O. K., & Glasgow, B. J. (2007). ANS fluorescence: potential to augment the identification of the external binding sites of proteins. *Biochimica et Biophysica Acta (BBA)-Proteins and Proteomics*, 1774, 403-411. <https://doi.org/10.1016/j.bbapap.2007.01.002>

Gómez-López, V. M., & Bolton, J. R. (2016). An approach to standardize methods for fluence determination in bench-scale pulsed light experiments. *Food and Bioprocess Technology*, 9, 1040-1048. <http://doi:10.1007/s11947-016-1696-z>.

Gómez-López, V. M., Ragaert, P., Debevere, J., & Devlieghere, F. (2007). Pulsed light for food decontamination: a review. *Trends in Food Science & Technology*, 18, 464-473. <https://doi.org/10.1016/j.tifs.2007.03.010>

Innocente, N., Segat, A., Manzocco, L., Marino, M., Maifreni, M., Bortolomeoli, I., & Nicoli, M. C. (2014). Effect of pulsed light on total microbial count and alkaline phosphatase activity of raw milk. *International Dairy Journal*, 39, 108-112. <https://doi.org/10.1016/j.idairyj.2014.05.009>

Ionitã, E., Stãnciuc, N., Aprodu, I., Rãpeanu, G., & Bahrim, G. (2014). pH-induced structural changes of tyrosinase from *Agaricus bisporus* using fluorescence and *in silico*

methods. *Journal of the Science of Food and Agriculture*, 94, 2338-2344.

<https://doi.org/10.1002/jsfa.6574>

Janve, B. A., Yang, W., Marshall, M. R., Reyes-De-Corcuera, J. I., & Rababah, T. M. (2014). Nonthermal inactivation of soy (*Glycine max* sp.) lipoxygenase by pulsed ultraviolet light. *Journal of Food Science*, 79, C8-C18. <https://doi.org/10.1111/1750-3841.12317>

Jiang, Y., Su, J. T., Zhang, J., Wei, X., Yan, Y. B., & Zhou, H. M. (2008). Reshaping the folding energy landscape of human carbonic anhydrase II by a single point genetic mutation Pro237His. *The International Journal of Biochemistry & Cell Biology*, 40, 776-788. <https://doi.org/10.1016/j.biocel.2007.10.022>

Ju, Z. Y., & Kilara, A. (1998). Aggregation induced by calcium chloride and subsequent thermal gelation of whey protein isolate. *Journal of Dairy Science*, 81, 925-931. [https://doi.org/10.3168/jds.S0022-0302\(98\)75652-8](https://doi.org/10.3168/jds.S0022-0302(98)75652-8)

Katayama, D. S., Nayar, R., Chou, D. K., Campos, J., Cooper, J., Vander Velde, D. G., Villarete, L., Liu, C.P., & Cornell Manning, M. (2005). Solution behavior of a novel type 1 interferon, interferon- τ . *Journal of Pharmaceutical Sciences*, 94, 2703-2715. <https://doi.org/10.1002/jps.20461>

Kuznetsova, I. M., Turoverov, K. K., & Uversky, V. N. (2004). Use of the phase diagram method to analyze the protein unfolding-refolding reactions: fishing out the “invisible” intermediates. *Journal of Proteome Research*, 3, 485-494. <http://doi.org/10.1021/pr034094y>

Malvezzi-Campeggi, F., Rosato, N., Finazzi-Agrò, A., & Maccarrone, M. (2001). Effect of denaturants on the structural properties of soybean lipoxygenase-1. *Biochemical and Biophysical Research Communications*, 289, 1295-1300. <https://doi.org/10.1006/bbrc.2001.6109>

Manzocco, L., Panozzo, A., & Nicoli, M. C. (2013a). Inactivation of polyphenoloxidase by pulsed light. *Journal of Food Science*, 78, E1183-E1187. <https://doi.org/10.1111/1750-3841.12216>

Manzocco, L., Panozzo, A., & Nicoli, M. C. (2013b). Effect of pulsed light on selected properties of egg white. *Innovative Food Science & Emerging Technologies*, 18, 183-189. <https://doi.org/10.1016/j.ifset.2013.02.008>

Micsonai, A., Wien, F., Kernya, L., Lee, Y. H., Goto, Y., Réfrégiers, M., & Kardos, J. (2015). Accurate secondary structure prediction and fold recognition for circular dichroism spectroscopy. *Proceedings of the National Academy of Sciences*, 2, E3095-E3103. <https://doi.org/10.1073/pnas.1500851112>

Minor, W., Steczko, J., Stec, B., Otwinowski, Z., Bolin, J. T., Walter, R., & Axelrod, B. (1996). Crystal structure of soybean lipoxygenase L-1 at 1.4 Å resolution. *Biochemistry*, 35, 10687-10701. <http://doi.org/10.1021/bi960576u>

Oliver, C. N., Ahn, B. W., Moerman, E. J., Goldstein, S., & Stadtman, E. R. (1987). Age-related changes in oxidized proteins. *Journal of Biological Chemistry*, 262, 5488-5491.

PDB 2019. 1YGE, lipoxygenase-1 (soybean) at 100K. <https://www.rcsb.org/pdb/explore/remediatedSequence.do?structureId=1YGE>. Accessed 11 April 2019.

Pellicer, J. A., & Gómez-López, V. M. (2017). Pulsed light inactivation of horseradish peroxidase and associated structural changes. *Food Chemistry*, 237, 632-637. <https://doi.org/10.1016/j.foodchem.2017.05.151>

Pellicer, J. A., Navarro, P., & Gómez-López, V. M. (2018). Pulsed light inactivation of mushroom polyphenol oxidase: a fluorometric and spectrophotometric study. *Food and Bioprocess Technology*, 11, 603-609. <https://doi.org/10.1007/s11947-017-2033-x>

Pellicer, J. A., Navarro, P., & Gómez-López, V. M. (2019). Pulsed light inactivation of polygalacturonase. *Food Chemistry*, *271*, 109-113.

<https://doi.org/10.1016/j.foodchem.2018.07.194>

Shriver, S. K., & Yang, W. W. (2011). Thermal and nonthermal methods for food allergen control. *Food Engineering Reviews*, *3*, 26-43. [https://doi.org/10.1007/s12393-011-9033-](https://doi.org/10.1007/s12393-011-9033-9)

[9](https://doi.org/10.1007/s12393-011-9033-9)

Siddique, M. A. B., Maresca, P., Pataro, G., & Ferrari, G. (2016). Effect of pulsed light treatment on structural and functional properties of whey protein isolate. *Food Research International*, *87*, 189-196. <https://doi.org/10.1016/j.foodres.2016.07.017>

Siddique, M. A. B., Maresca, P., Pataro, G., & Ferrari, G. (2017). Influence of pulsed light treatment on the aggregation of whey protein isolate. *Food Research International*, *99*, 419-425. <https://doi.org/10.1016/j.foodres.2017.06.003>

Sigma-Aldrich (2019). Lipoxidase preparation from *Glycine max* (soybean). https://www.sigmaaldrich.com/content/dam/sigma-aldrich/docs/Sigma/Product_Information_Sheet/2/17395pis.pdf. Accessed 28 May 2019.

Stănciuc, N., Aprodu, I., Râpeanu, G., & Bahrim, G. (2012). Fluorescence spectroscopy and molecular modeling investigations on the thermally induced structural changes of bovine β -lactoglobulin. *Innovative Food Science & Emerging Technologies*, *15*, 50-56. <https://doi.org/10.1016/j.ifset.2012.03.001>

Sudharshan, E., & Rao, A. A. (1999). Involvement of cysteine residues and domain interactions in the reversible unfolding of lipoxygenase-1. *Journal of Biological Chemistry*, *274*, 35351-35358. <http://doi.org/10.1074/jbc.274.50.35351>

Youn, B., Sellhorn, G. E., Mirchel, R. J., Gaffney, B. J., Grimes, H. D., & Kang, C. (2006). Crystal structures of vegetative soybean lipoxygenase VLX-B and VLX-D, and

comparisons with seed isoforms LOX-1 and LOX-3. *Proteins: Structure, Function, and Bioinformatics*, 65, 1008-1020. <https://doi.org/10.1002/prot.21182>

Wang, B., Zhang, Y., Venkitasamy, C., Wu, B., Pan, Z., & Ma, H. (2017). Effect of pulsed light on activity and structural changes of horseradish peroxidase. *Food Chemistry*, 234, 20-25. <http://dx.doi.org/10.1016/j.foodchem.2017.04.149>.

FIGURE CAPTIONS

Figure 1. Inactivation of lipoxygenase by pulsed light treatment. Inset: Weibull fitted curve. Bars represent standard deviation (n=3).

Figure 2. Electrophoresis of LOX at increasing fluence during the course of PL treatment.

Figure 3. (a) Far-UV circular dichroism at different fluences (J/cm^2) and (b) relative content of secondary structures of native and PL treated LOX.

Figure 4. Evolution of intrinsic fluorescence parameters during the course of PL treatment of LOX. (a) Fluorescence spectrum **at different fluences (J/cm^2)**, (b) spectral center of mass, (c) parameter A and (d) phase diagram.

Figure 5. ANS fluorescence of LOX at increasing fluence (J/cm^2) during the course of PL treatment and unbound ANS fluorescence.

Table 1. Change in temperature, aggregation index and turbidity during the course of LOX inactivation by PL.

Fluence (J/cm ²)	Temperature (°C)	Aggregation index (---) ¹	Turbidity (Abs. 420 nm)
0.0	24.5±1.1	4.23±2.23 ^a	0.005±0.004 ^a
10.7	25.4±1.0	6.58±3.02 ^a	0.009±0.005 ^{ab}
21.4	26.6±0.7	7.49±2.45 ^{ab}	0.009±0.004 ^{ab}
32.1	27.5±1.0	9.16±2.38 ^{abc}	0.011±0.004 ^{ab}
42.8	28.4±1.3	10.69±2.04 ^{abcd}	0.013±0.003 ^{ab}
53.5	28.8±1.1	11.92±1.91 ^{abcd}	0.014±0.003 ^{ab}
64.2	29.2±1.2	14.70±2.95 ^{bcd}	0.019±0.004 ^b
74.9	29.5±1.2	15.32±3.17 ^{cd}	0.018±0.006 ^b
85.6	29.7±1.2	16.52±3.29 ^{cd}	0.019±0.007 ^b
96.3	30.0±1.3	18.03±3.03 ^d	0.020±0.006 ^b

¹ Dimensionless.

Table 2. Change in free sulfhydryl's and carbonyl content during the course of LOX inactivation by PL.

Fluence (J/cm ²)	Free sulfhydryl's (µmol/g prot.)	Carbonyls (mmol/mg prot.)
0.0	4.14±1.80 ^a	0.013±0.000 ^a
32.1	8.55±1.27 ^b	0.016±0.001 ^a
64.2	10.55±1.36 ^b	0.030±0.003 ^b
96.3	12.09±0.81 ^b	0.063±0.005 ^c

Figure 1

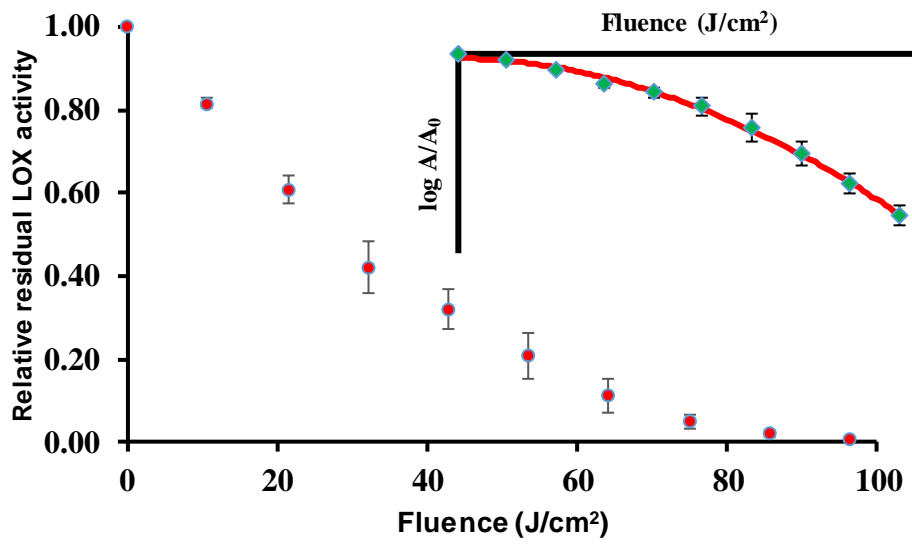


Figure 2

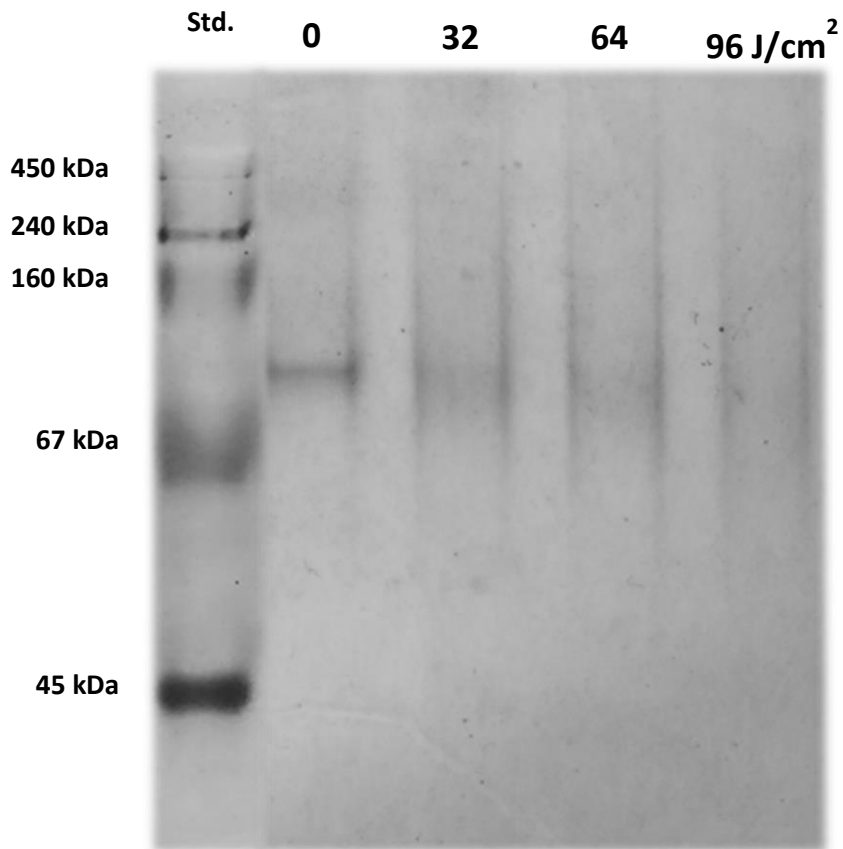


Figure 3

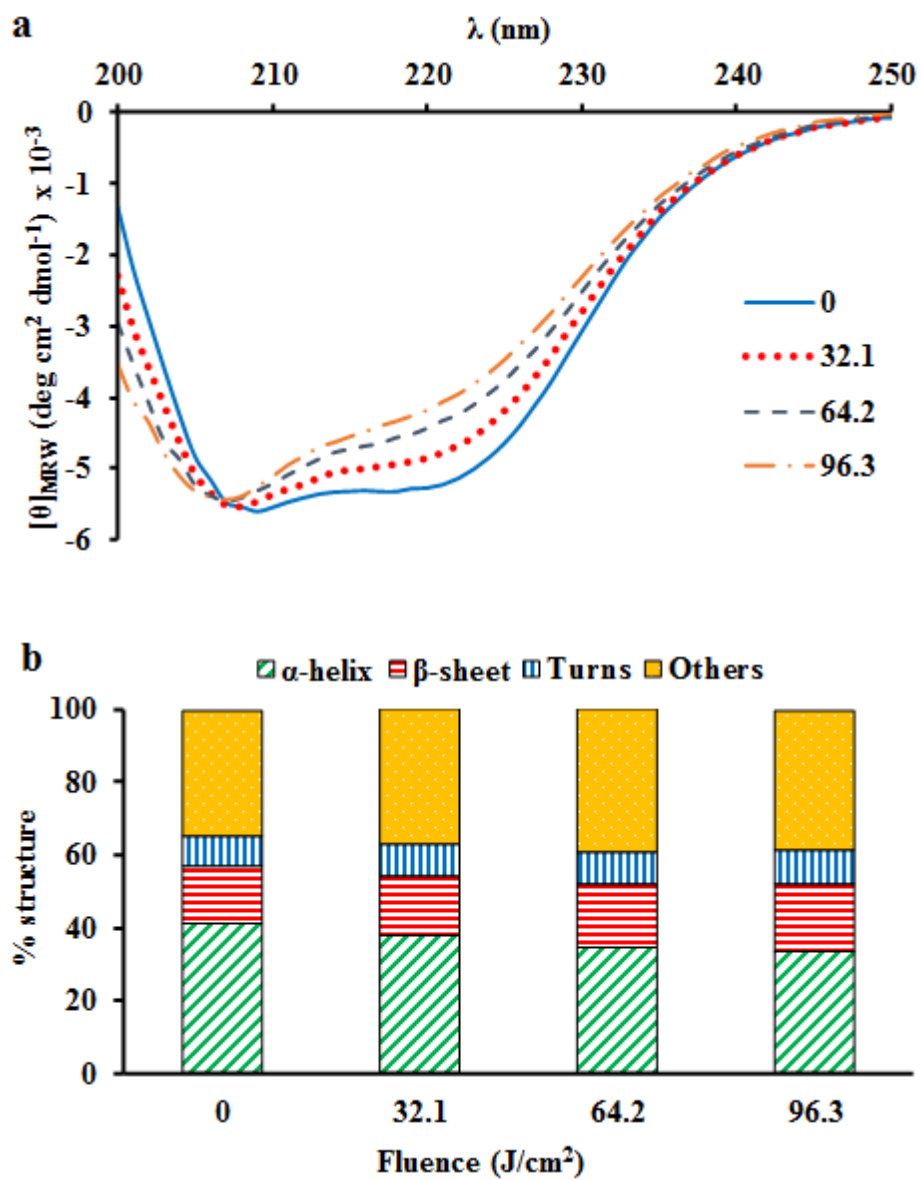


Figure 4

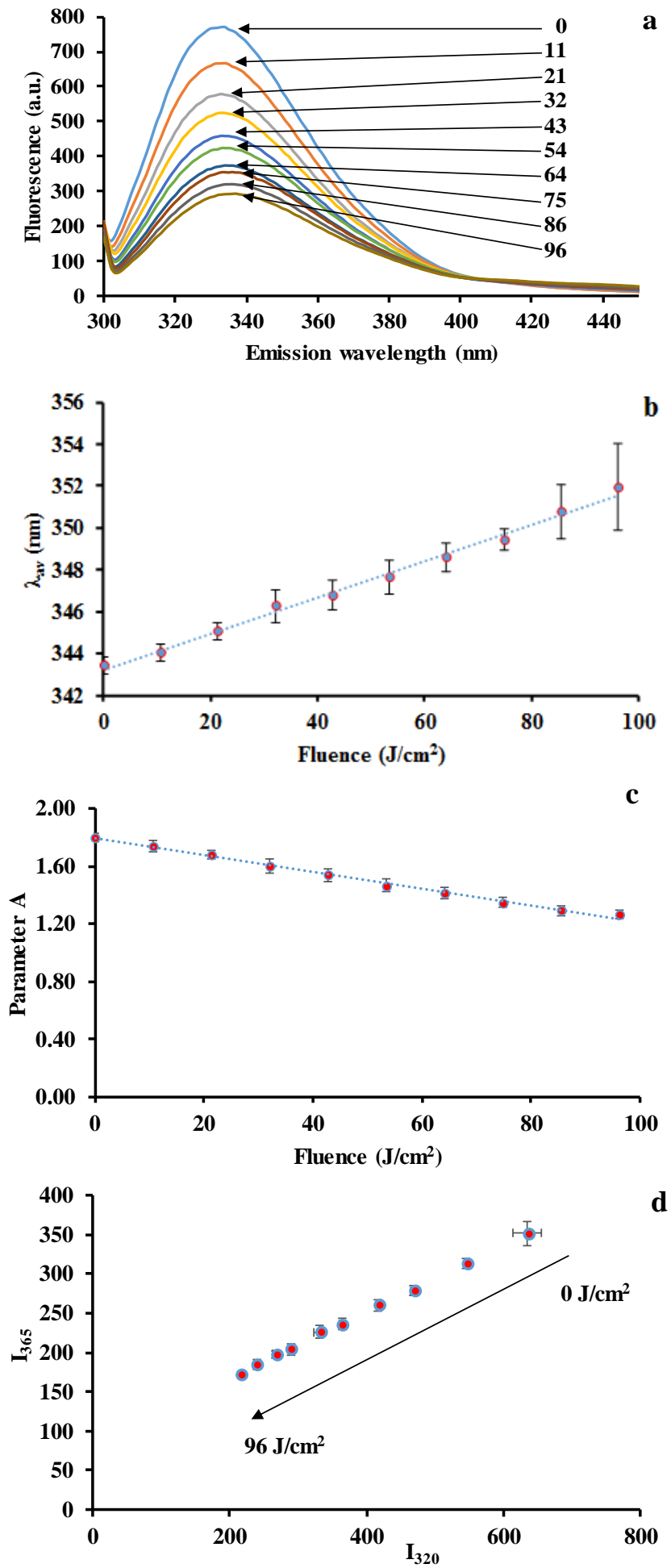


Figure 5

